Controlled anisotropic growth of Ag nanoparticles on oil-decorated TiO_2 films with photocatalytic reduction method

Shuai Li, Qiang Tao, Dawei Li, and Qingyu Zhang[a)]
Key Laboratory of Materials Modification by Laser, Ion and Electron Beams, School of Physics & Optoelectronic Technology, Dalian University of Technology, Dalian 116024, China

(Received 3 April 2014; accepted 10 September 2014)

Ag–TiO_2 hybrids are useful in various applications, such as photocatalysis, solar energy conversion, and biosensoring. In this study, oil-decorated TiO_2 films were used to induce the formation of Ag nanoplates in $AgNO_3$ solution via a photocatalytic method. Ag nanoplates in the products can be controlled by changing the oil-decoration time of films or changing the $AgNO_3$ concentration of the solution. Oil decoration was found to be necessary in the formation of Ag nanoplates, and a critical concentration of $AgNO_3$ solution was needed. The oil layer on the TiO_2 films was demonstrated to play a role in the prevention of the reoxidation of the Ag atoms, and a growth model was proposed to interpret the formation of Ag nanoplates on the oil-decorated TiO_2 films.

I. INTRODUCTION

TiO_2 is the most promising material in the field of photocatalysis because of its superior photocatalytic activity, chemical stability, low cost, and nontoxicity. As such, its performances in the photodegradation of chemical pollutants and solar energy conversion have been extensively studied in the past decades, and its practical application has been seriously considered.[1,2] TiO_2 assembled with noble metal nanocomposite particulates has received much attention, because such a hybrid can effectively separate the charges and redshift the absorption to visible light via plasmonic resonance on the metal nanoparticle.[3–5] For example, Awazu et al. combined TiO_2 and Ag core/SiO_2-shell nanoparticles in a heterostructure and the photocatalytic activity was enhanced by a factor of 7 under near-ultraviolet (UV) irradiation.[4] TiO_2 assisted by the localized surface plasmonic resonance (LSPR) of Ag NPs is promising in applications such as photocatalysis,[3–5] solar cells,[6,7] reversible imaging,[8] and LSPR sensors.[9]

Many methods have been used to assemble metal nanoparticles (NPs) onto a solid surface, and some of the top-to-down lithographic methods (e.g., electron-beam lithography, nanoprint lithography, and nanosphere lithography) have been used to control the growth of metal NPs. The photocatalytic reduction method is a cost-effective and facile method to synthesize Ag NPs on TiO_2 film. Under UV irradiation, Ag NPs are directly grown on the TiO_2 film by reducing Ag^+ ions in $AgNO_3$ solution. However, the as-grown Ag NPs on TiO_2 films are often sphere-like, and an effective method is still needed for controlling the formation of anisotropic Ag NPs with the photocatalytic reduction method. It is well known that LSPR gives rise to absorption and scattering of light at specific wave lengths, which depends on the particle size, shape, orientation, interparticle spacing, and dielectric environment.[10–13] A controlled anisotropic growth of Ag NPs on TiO_2 films is expected in tuning the optical response of the Ag–TiO_2 hybrid films. Moreover, the growth behavior of the Ag NPs on TiO_2 films has also attracted a fundamental interest. Recently, the photocatalytic growth of anisotropic Ag NPs on the nanoparticulate TiO_2 films in the $AgNO_3$ ethanol solution was reported, and the vertical growth of Ag nanoplates was attributed to the surface roughness and random features of the substrate.[14,15] Using an annealed single-crystalline TiO_2 substrate, Kazuma et al.[16] reported the bi- and uniaxially oriented growth of Ag NPs. They found that the preferential orientation and morphology of these Ag NPs depend on the presence of ethanol, acetaldehyde, and UV exposure conditions. However, the anisotropic growth of the Ag NPs on TiO_2 films in an $AgNO_3$ solution without an organic agent has not been reported.

In our previous study, the thickness of TiO_2 films was used to control the photocatalytic growth of the Ag NPs.[17] Isotropic Ag NPs with controlled size and density were obtained. The reported method was demonstrated to be valid for the controlled design of the TiO_2-catalyzed Ag NP films, but Ag NPs with well-defined shapes were not synthesized. In this paper, we report a photocatalytic method to grow Ag nanoplates on TiO_2 films in $AgNO_3$ solution. Oil-decorated TiO_2 film was used to induce the anisotropic growth of Ag NPs. Scanning electron microscopy (SEM), high-resolution

[a)]Address all correspondence to this author.
e-mail: qyzhang@dlut.edu.cn
DOI: 10.1557/jmr.2014.283

transmission electron microscopy (HRTEM), and in situ extinction spectra were used to investigate the growth behaviors of the Ag NPs on TiO_2 films with and without oil decoration. The growth behaviors are also discussed in the terms of Ostwald ripening (OR) and oriented attachment (OA).

II. EXPERIMENTAL

A. Preparation of TiO_2 films

The nanoparticulate TiO_2 films used for the growth of Ag NPs were prepared using a conventional sol–gel method. First, solutions A and B were prepared by mixing 3 mL acetylacetone with 50 mL titanium isopropoxide and by adding 0.21 mL nitric acid and 1.4 mL deionized water into 150 mL ethyl alcohol, respectively. All the chemicals used in the preparation of solutions A and B were analytical reagents and were purchased from Kermel Chemical Reagents Co. Ltd. Both the mixtures were stirred for 10 min. Subsequently, the TiO_2 sol was prepared by adding solution B dropwise into solution A under vigorous stirring. After mixing, the TiO_2 sol was stirred for 2 h at room temperature and aged for 2 days before use. Finally, the TiO_2 gel films were coated on the substrate of a cleaned glass slide via the dip-coating method. The TiO_2 gel films were heated at 550 °C for 1 h in a muffle furnace to obtain the nanoparticulate TiO_2 films. The TiO_2 films were controlled at ~200 nm. The TiO_2 films, which were immediately used in 1 h after calcining for the growth of Ag NPs, were defined as the fresh films in this paper.

To realize the anisotropic growth of Ag NPs, the TiO_2 film was modified by coating a layer of vacuum pump oil (>90% hydrocarbons, Huifeng Petroleum and Chemical Co. Ltd.). In this paper, the modified film has been referred to as the oil-decorated film. The oil-decorated films were prepared by evaporating the oil on the fresh films. In the preparation, the oil was heated to ~98 °C and the fresh films were placed at a ~15 cm distance from the oil, toward the oil bath. The time of oil decoration was controlled at 1, 2, 4, and 8 min, respectively. The number of oil molecules on the film was estimated using surface enhanced Raman scattering (SERS), which is capable of detecting the ultratrace molecules. Raman signals were collected with a Raman spectroscope (Renishaw inVia plus, Renishaw, Wotton-under-Edge Gloucestershire, UK). Water contact angle was also used for characterizing the surface properties of the films with and without oil decoration.

B. Growth and characterization of Ag NPs

Ag NPs were grown in $AgNO_3$ aqueous solution under irradiation by a low-pressure mercury lamp (Philips TUV, 8 W, Amsterdam, Netherlands). The growth of the Ag NPs was monitored by measuring the in situ extinction spectra with UV–visible-near-infrared spectrometer (UV–Vis-NIR) (Ocean Optics, Maya 2000-Pro, Dunedin, FL). SEM (Hitachi, S-4800, Tokyo, Japan) was used to examine the morphology of the Ag–TiO_2 films. The Ag NPs in the SEM images were statistically analyzed to obtain the size distribution. HRTEM (TECNAI G^2, FEI, Hillsboro, OR) was used to study the crystallographic relationship between the Ag NPs in contact. The HRTEM samples were prepared by stripping the Ag NPs from the TiO_2 films in water via ultrasonic method.

III. RESULTS AND DISCUSSION

Similar to our previous report,[17] the Ag NPs on the fresh films show the irregular spherical shapes of isotropic growth, irrespective of the $AgNO_3$ concentration, which ranged from 200 to 3200 mg/L (1.2–19.2 mM) in this study. Figure 1(a) depicts a typical SEM image and the corresponding size distribution of Ag NPs. The sizes of the Ag NPs were defined as the square root of the cross-sectional area of the Ag NP SEM images. For comparison, the SEM image of the bare TiO_2 film is also presented in the inset at the bottom-left corner of Fig. 1(a). We found that the asymmetric distribution of the Ag NPs' size can be well fitted with the extreme function, $y = A\exp(-\exp(-z) + z + 1)$, where y is the percentage of the Ag NPs with the size of x, $z = (x - x_c)/\sigma$, x_c Ag NP feature size at the most probable value, and σ is the standard deviation. The feature size (x_c) is ~80 nm at 5 min growth time, as shown in the inset at the top-right corner of Fig. 1(a). With the increase in growth time (t), the feature size is on the increase, as shown in Fig. 1(b). The average size (d) of Ag NPs fit the relation $d^3 - d_0^3 = kt$, indicating that OR mechanism dominates the crystal growth of Ag NPs.[18] Such Ag–TiO_2 hybrids have been reported in the photocatalytic synthesis of Ag NPs and adopted in the studies related to LSPR-assisted TiO_2 photocatalysis and SERS.[17,19–23]

Under the same growth condition as the case in Fig. 1, the growth behavior of Ag NPs on the oil-decorated TiO_2 films was varied, as shown in Fig. 2. In the initial growth stage (at 1 min), Ag NPs show sphere-like shapes that are similar to those grown on the fresh films, but their sizes are smaller. By increasing the growth time to 2 and 4 min, the anisotropic Ag NPs, or the small Ag nanoplates, appear in the products. At 8 min growth time, the well-defined Ag nanoplates, upright standing or tiled, were popularly observed in the product. The formation of Ag nanoplates is likely due to the aggregation of the primary particles (nuclei) in the nucleation stage. As indicated by the circles in the figure, the spherical Ag NPs in some regions aggregate together or form Ag nanochains, as shown in Figs. 2(a) and 2(b), and then the small Ag nanoplates are gradually developed to be the perfect regular

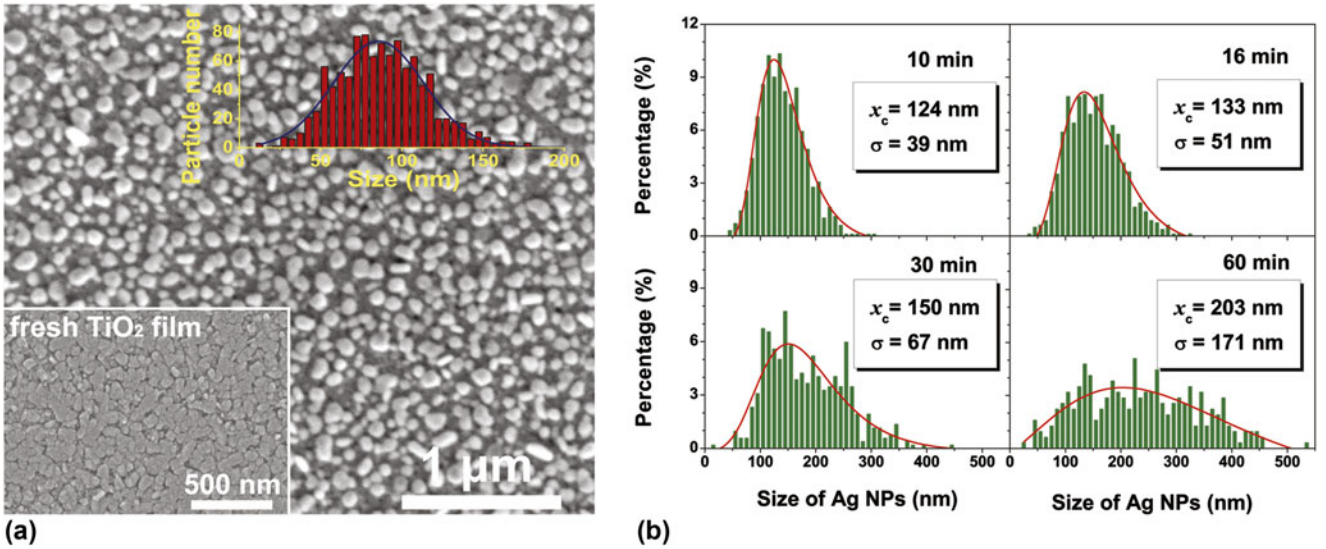

FIG. 1. Typical SEM image (a) and the size distribution (b) of Ag NPs grown on fresh TiO_2 films in the $AgNO_3$ solution of 3200 mg/L. The insets at the bottom-left and top-right corners of Fig. 1(a) are the SEM image of the bare TiO_2 film and the size distribution of Ag NPs at the growth time of 5 min, respectively.

triangles or hexagons, as shown in Figs. 2(c) and 2(d). Such nanoplates have three major LSPR modes, namely, out-of-plane mode and in-plane longitudinal and transverse modes, and respond selectively to light polarized in a specific angle. Thereby, the Ag nanoplates can be applied to the fields such as stereoscopic visions, storing multiple information, certification, and anticounterfeit technologies and polarizers.[24,25] Using the upright standing and the tiled Ag nanoplates, the thickness of the Ag nanoplates was estimated to be 30–40 nm, whereas the lengths of their edges ranged from 0.1 to 1 μm. TEM analysis reveals that the Ag nanoplates are faced with (111) planes. The above results indicate that the oil-decorated TiO_2 films successfully induce the anisotropic growth of Ag NPs.

Figure 3 shows the size distributions of the Ag NPs on the oil-decorated films at the growth times of 1, 2, 4, and 8 min. Initially, the size distribution of the Ag NPs on the oil-decorated films is similar to that of the Ag NPs on the fresh films, as shown in Fig. 3(a). With an increase in the growth time, the feature size of the distribution does not obviously increase, but the percentage of large Ag NPs increases considerably, forming a distribution tail, as shown in Figs. 3(b)–3(e). This type of evolution is much different from that of Ag NPs on the fresh films. When compared with the SEM images in Fig. 2, the feature sizes were found to be determined by the distributions of irregularly spherical Ag NPs in the products, and the appearance of the Ag nanoplates results in the formation of distribution tails. Because the feature size was not increased by increasing the growth time, we conclude that the isotropic growth of Ag NPs on the oil-decorated films is restrained. The change in growth

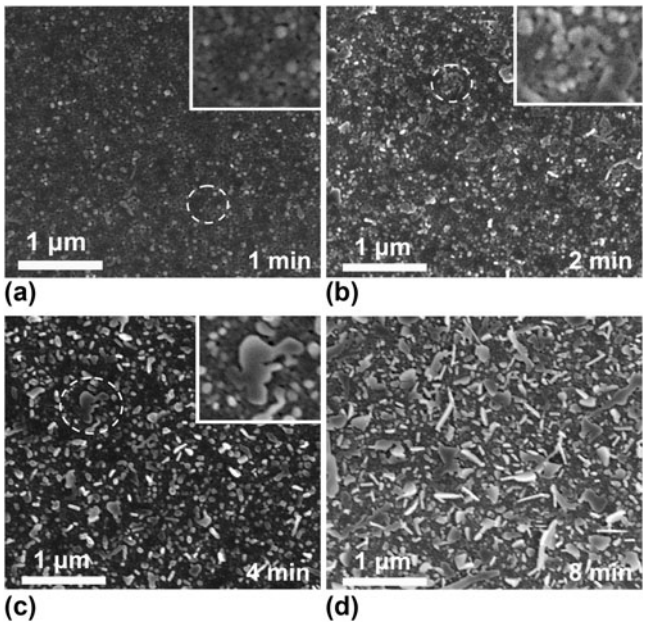

FIG. 2. (a–d) SEM images of Ag NPs grown on the oil-decorated TiO_2 films in the $AgNO_3$ solution of 3200 mg/L at the given growth times. The insets are the enlarged SEM images of the encircled regions in the figures.

behavior was also observed in the in situ extinction spectra, as shown in Fig. 3(f). The extinction intensities in the visible region slowly increase by increasing the growth time, whereas the extinction in the NIR region is quickly enhanced. The small peak at ~340 nm, which was first observed at 8 min, is due to the out-of-plane quadrupole resonance of the Ag nanoplates in $AgNO_3$ solution, and the peak position is associated with the

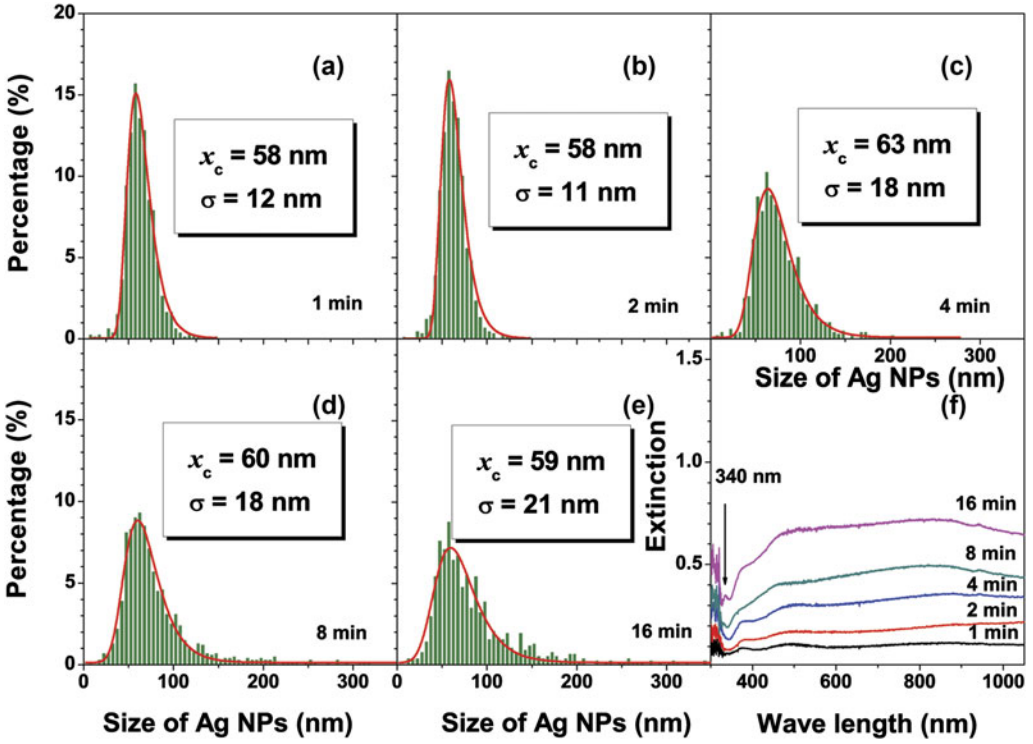

FIG. 3. (a–e) Size distribution of Ag NPs grown on the oil-decorated TiO_2 films in the $AgNO_3$ solution of 3200 mg/L and (f) the corresponding extinction spectra.

thickness of the Ag nanoplates.[13] According to the effective medium theory,[26,27] isotropic Ag NPs contribute to the extinction in the visible region and Ag nanoplates give rise to an enhancement of the extinction in the NIR region. Thereby, we also conclude that the oil-decorated films play a role in restraining the isotropic growth of the Ag NPs.

The Ag nanoplates in the product were found to be dependent on the oil-decoration time of the TiO_2 film. Figure 4 shows the SEM images of the Ag NPs grown on the TiO_2 films with their corresponding time of oil decoration. The 3200 mg/L $AgNO_3$ solution was used, and the growth time was controlled at 5 min. The number of Ag nanoplates increases with an increase in the oil-decoration time until 4 min, and then no obvious difference is observed. In addition, we found that a shorter time of oil decoration leads to the production of smaller Ag nanoplates. Besides the oil-decoration time, the $AgNO_3$ concentration is found to be important in determining the formation of Ag nanoplates on the oil-decorated films. Figure 5 shows the SEM images of Ag NPs grown on the oil-decorated films in the 1600, 800, 400, and 200 mg/L $AgNO_3$ solutions, in which Ag NPs were grown in solution for 6 min and the oil-decoration time of TiO_2 film was 4 min. Ag nanoplates cannot be synthesized in the $AgNO_3$ solution below 200 mg/L. In $AgNO_3$ solutions with concentration >400 mg/L, the density of the Ag nanoplates increases with an increase in the $AgNO_3$ concentration, indicating that

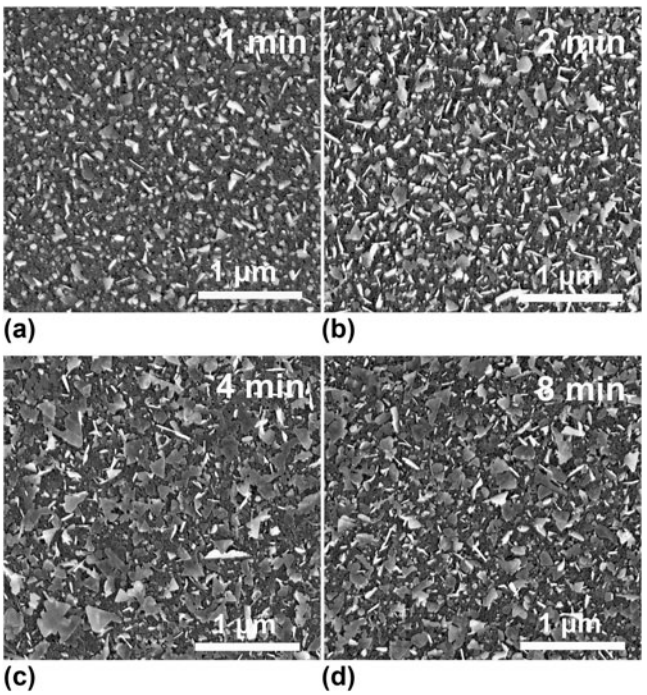

FIG. 4. SEM images of Ag NPs grown on the films with oil decoration of 1, 2, 4, and 8 min, with the use of 3200 mg/L $AgNO_3$ solution at 5 min growth time.

a critical $AgNO_3$ concentration is required for the formation of Ag nanoplates on the oil-decorated films. In this study, the critical $AgNO_3$ concentration is

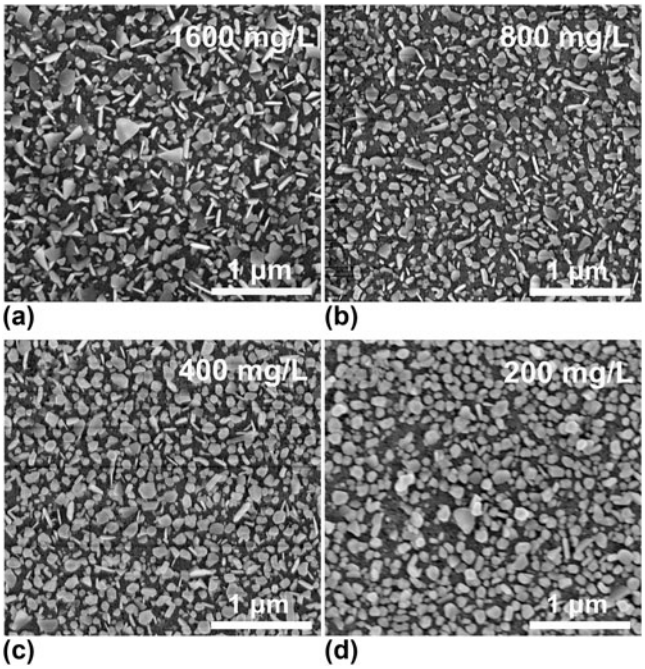

FIG. 5. SEM images of Ag NPs grown on the oil-decorated films in the $AgNO_3$ solutions of 1600, 800, 400, and 200 mg/L; the growth time is 6 min and the time of oil decoration is 4 min.

between 200 and 400 mg/L. We found that the critical concentration is necessary to induce the formation of Ag nanoplates on the oil-decorated films, irrespective of the decoration time.

To characterize the surface change, the water contact angles of the films were measured. The contact angle of water on the fresh film is ~6°, and it increases to 12°, 23°, 27°, and 33° for the films with oil decoration of 1, 2, 4, and 8 min, respectively, evidencing that the surface properties of the films were modified by oil decoration. Because oil molecules are easily desorbed in ultrahigh vacuum at room temperature, they cannot be characterized with the conventional surface analysis methods, such as x-ray photoelectron spectroscopy and Auger electron spectroscopy. Therefore, SERS was used to estimate the number of oil molecules on the films. To be reliable, three kinds of SERS samples, namely, oil-decorated Ag NPs on fresh film (S1), Ag NPs on oil-decorated TiO_2 film (S2), and Ag NPs on fresh film (S3), were prepared for the Raman spectrum comparison with the pump oil in capillary. Sample S1 was made by evaporating the pump oil onto Ag NPs grown on fresh films. Samples S2 and S3 were Ag NPs grown on TiO_2 films with and without oil decoration, respectively. As shown in Fig. 6, the Raman peaks of C–H bonds in the range of 2800–3000 cm^{-1} were detected for the samples with oil molecules (S1 and S2), but no Raman signal was detected for the oil-free sample (S3). Thus, the detected Raman signals are attributed to the oil decoration.

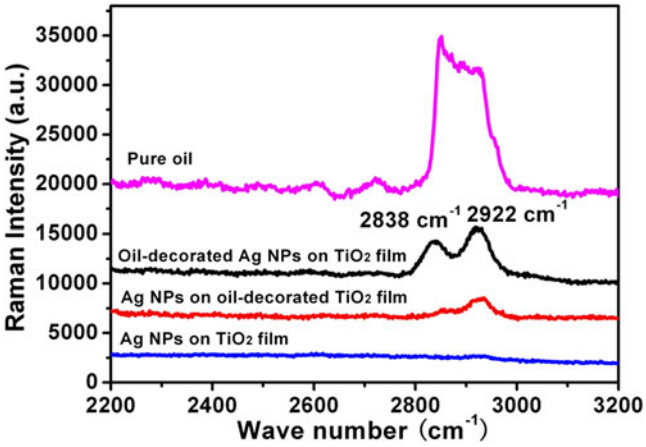

FIG. 6. Raman spectra of the pump oil in capillary and those taken from the samples of the TiO_2 films with and without oil decoration as indicated in the figure.

As all organic solvents exhibit the same Raman peaks of C–H bonds as the oil, the number of oil molecules on the films can only be estimated using SERS enhanced factors (EF) of the Ag–TiO_2 film, which was determined using a certain concentration of rhodamine 6G as the probe. In this study, 1 μM rhodamine 6G ethanol solution was used. Assuming that the determined SERS EF was valid for the oil-decorated samples, we obtained 10^{15}–10^{16} cm^{-2} of C–H bond density using the Raman intensity of the pump oil in capillary as the reference. Because such an estimation depends on the probe concentration, photodegradation of methylene blue, which is discussed in the following text, was also used for the estimation by supposing the photodegradation rate of oil molecules on TiO_2 film to be the same as that of methylene blue in solution, and ~10^{16} C–H/cm^2 per minute of oil deposition rate was obtained. The two methods resulted in approximately the same conclusion that a sublayer to a few layers of oil molecules was deposited on the TiO_2 film after oil decoration.

The above results prove that the oil-decorated films are capable of promoting the anisotropic growth of Ag NPs in the photocatalysis, and the oil layer on the films is responsible for the formation of Ag nanoplates. However, obtaining direct evidence to reveal the oil-layer function in the formation of Ag nanoplates is difficult because the growth of Ag NPs is a dynamic process, and no available technique can be used for an in situ observation of the Ag NP growth. Based on our observation, nucleation theory, and photocatalysis principle, a simple discussion on the growth of Ag NPs on the oil-decorated films is presented.

First, two kinds of Ag NPs, isotropic NPs (~60 nm size) and anisotropic nanoplates (30–40 nm thickness), were obtained using the oil-decorated films. However, the initial nucleation of Ag NPs on the oil-decorated films

is similar to that on the fresh film except that the size of the primary particle is smaller. According to the nucleation theory of crystal growth,[28] high supersaturation of the neutral atom leads to the small size and high density of the primary particles (nuclei). Thereby, the formation of Ag nanoplates is related to the increase in the density of Ag atoms. In other words, the reduction rate of Ag atoms on the oil-decorated films is likely higher than that on the fresh film. The critical $AgNO_3$ concentration for the formation of Ag nanoplates also suggests that the anisotropic growth needs a high Ag reduction rate, which is proportional to the concentration of Ag ions in solution. The increase in the Ag reduction rate can be attributed to the efficient charge separation of photocatalysis due to the introduction of the oil layer on TiO_2 films. As is well-known, two kinds of photoinduced carriers, electron and hole, are generated in the TiO_2 film and are transferred to its surface. The electron reduces the ions in solution and the hole oxidates the neutral particles into ions. Thus, the reoxidation of the reduced Ag atoms decreases the Ag reduction rate. We believe that the oil layer on the TiO_2 film is the substitute for the reduced Ag atoms. Because the Ag atoms avoid reoxidation with the oil layer, the net reduction rate of the Ag atoms is increased.

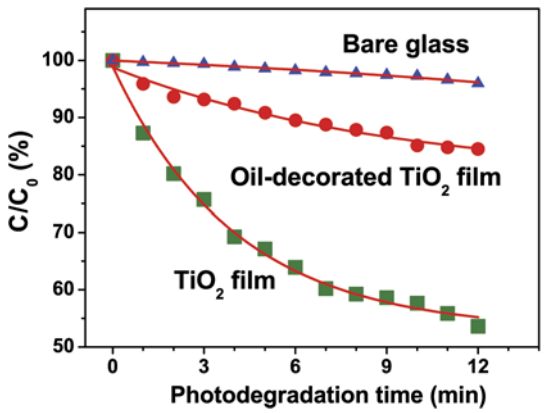

FIG. 7. Photodegradation curves of methylene blue aqueous solution obtained by using the samples of fresh TiO_2 film, oil-decorated TiO_2 film, and bare glass. The initial solution concentration (C_0) was 10 mg/L, and the concentration (C) of methylene blue in photodegradation was determined by using the absorption spectra collected. A low-pressure mercury lamp was used as the irradiation source for the photodegradation.

To demonstrate our assumption, the photodegradation of 10 mg/L methylene blue aqueous solution was compared using three samples, namely, the fresh film, the oil-decorated TiO_2 film, and a bare glass, as shown in Fig. 7. The fresh film exhibits the highest photodegradation rate. After oil decoration, the photodegradation is considerably reduced, indicating that the oil layer prevents the oxidation of methylene blue. The glass sample shows the lowest photodegradation rate of methylene blue, which can be attributed to the UV-induced photodegradation. The experiments clearly demonstrated that the oil layer is capable of preventing oxidation of the Ag atoms in the growth of Ag NPs, leading to the increase in the density of Ag atoms. An interesting phenomenon in using the oil-decorated films is that the photodegradation rate sharply increased at time $> \sim 15$ min, which is likely the time when the oil layer was consumed due to the photodegradation.

Second, we found that most of the Ag nanoplates pile up over each other or lay over the irregularly shaped Ag NPs, as shown in Figs. 4(c) and 4(d). In addition, these Ag nanoplates are mobile and easily stripped from the substrates. These observations suggest that the formation of Ag nanoplates likely took place in the area adjacent to the film surface, and they adhered to the surface when they were taken out from the solution. In other words, the Ag nanoplates probably originated from the self-nucleation of Ag NPs in the solution, but not from the heterogeneous nucleation on the TiO_2 film. However, studies involving the self-nucleation or heterogeneous nucleation of Ag NPs via photocatalytic reduction are unavailable. On the basis of the given observation, we suggest a scenario for the growth of Ag NPs via photocatalytic reduction with TiO_2 film, as shown in Fig. 8. Considering Ag atom mobility and reoxidation, a specific Ag atom distribution is suggested, as shown in

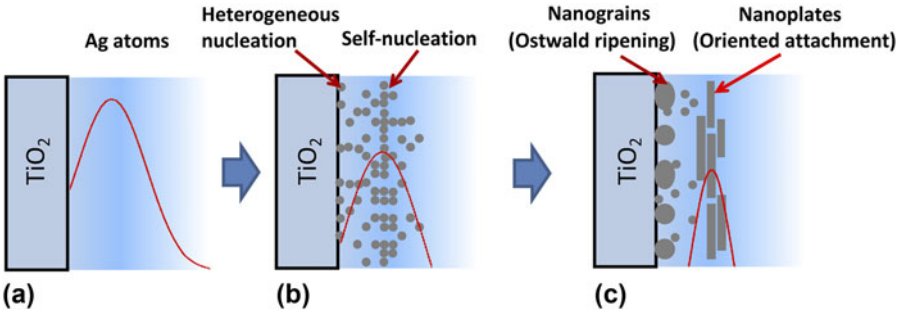

FIG. 8. Photocatalytic growth model of Ag NPs in $AgNO_3$ solution with TiO_2 films (a) reduction of Ag atoms, (b) nucleation of Ag primary particles, and (c) formation of Ag NPs or nanoplates.

Fig. 8(a). Depending on the nucleation free energy and the supersaturation, self-nucleation in the solution and heterogeneous nucleation on the film surface are both possible, as shown in Fig. 8(b). After nucleation, the Ag NPs grow through two mechanisms, OR and OA. The OR mechanism often leads to an isotropic growth, whereas the OA mechanism results in the formation of nanoplates, nanorods, and nanosheets, etc. We believe that the formation of the Ag nanoplates in this study is likely related to the OA growth.

The OA mechanism is a particle-mediated mesoscopic transformation process,[29,30] and has been demonstrated to be one of the important mechanisms leading to the anisotropic growth of Ag NPs in solution-phase synthesis. Yin et al.[31] found that both OA and OR mechanisms coexist in the growth of NPs. At the initial stage, increasing the concentration of the primary particles facilitates the OA-based growth, and the OR growth is restrained. Our observation with regard to the growth of Ag NPs is consistent with that by Yin et al. The HRTEM observation also implies that the OA growth is likely responsible for the formation of Ag nanoplates on the oil-decorated films. Figure 9 shows two typical images of Ag NPs in contact, which were stripped from the sample of Ag–TiO_2 hybrids at 8 min growth time. The contacted Ag NPs exhibit the lattice spacings of 0.24–0.25 nm, which are closed to the spacing of Ag (111) plane (0.2361 nm). Similar Ag NPs in contact were never observed on the fresh films. In the in situ HRTEM study of crystal growth controlled by the OA mechanism in solution-phase synthesis,[32] Li et al. took a series of TEM images of the NPs in contact, which are interpreted as the particles undergoing continuous rotation and interaction before they find a perfect match.

The proposed photocatalytic growth model helps us to understand the growth behavior of Ag NPs on TiO_2 films, and provide information on developing a more effective method to control the growth of Ag NPs. For example, we have tried to use TiO_2 films that were kept in air for weeks to grow Ag NPs, and a large amount of triangular and polygonal Ag NPs were obtained. This result suggests that the surface properties of TiO_2 films changed in a high-moisture environment. However, the surface-capping agents, such as polyvinylpyrrolidone (PVP), polyethylene glycol (PEG), sodium citrate, etc., were found to be useless in controlling the anisotropic growth of Ag NPs on TiO_2 films, possibly due to their high water solubility.

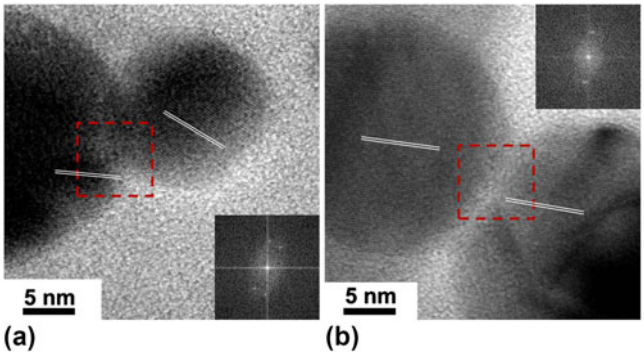

FIG. 9. Typical HRTEM images of contacted Ag NPs grown on the oil-decorated TiO_2 films in 3200 mg/L $AgNO_3$ solution.

IV. CONCLUSIONS

In conclusion, we developed a photocatalytic reduction method to control the crystal growth of Ag NPs in $AgNO_3$ solution. The upright standing or tiled Ag nanoplates were synthesized using the oil-decorated TiO_2 films. The growth of Ag nanoplates in the products can be controlled by changing the oil-decoration time and the $AgNO_3$ concentration. The increase in the reduction rate of Ag atoms caused by the introduction of the oil layer is suggested to be responsible for the formation of Ag nanoplates, which is likely due to the growth of Ag NPs dominated by the OA mechanism. The principle revealed in this study can be applied for the controlled assembly of Ag or other metal NPs on TiO_2 films via photocatalytic methods and is helpful in understanding the photocatalytic properties of TiO_2 films.

REFERENCES

1. M.R. Hoffmann, S.T. Martin, W. Choi, and D.W. Bahnemann: Environmental applications of semiconductor photocatalysis. *Chem. Rev.* **95**, 69 (1995).
2. X. Chen and S.S. Mao: Titanium dioxide nanomaterials: Synthesis, properties, modifications, and applications. *Chem. Rev.* **107**, 2891 (2007).
3. M. Es-Souni, M. Es-Souni, S. Habouti, N. Pfeiffer, A. Lahmar, M. Dietze, and C-H. Solterbeck: Brookite formation in TiO_2-Ag nanocomposites and visible light induced templated growth of Ag nanostructures in TiO_2. *Adv. Funct. Mater.* **20**, 377 (2010).
4. K. Awazu, M. Fujimaki, C. Rockstuhl, and J. Tominaga: A plasmonic photocatalyst consisting of silver nanoparticles embedded in titanium dioxide. *J. Am. Chem. Soc.* **130**, 1676 (2008).
5. W. Hou and S.B. Cronin: A review of surface plasmon resonance-enhanced photocatalysis. *Adv. Funct. Mater.* **23**, 1612 (2013).
6. Y. Tian and T. Tatsuma: Mechanisms and applications of plasmon-induced charge separation at TiO_2 films loaded with gold nanoparticles. *J. Am. Chem. Soc.* **127**, 7632 (2005).
7. Z. Liu, W. Hou, P. Pavaskar, M. Aykol, and S.B. Cronin: Plasmon resonant enhancement of photocatalytic water splitting under visible illumination. *Nano Lett.* **11**, 1111 (2011).
8. Y. Ohko, T. Tatsuma, T. Fujii, K. Naoi, C. Niwa, Y. Kubota, and A. Fujishima: Multicolour photochromism of TiO_2 films loaded with silver nanoparticles. *Nat. Mater.* **2**, 29 (2003).
9. I. Tanahashi, H. Iwagishi, and G. Chang: Localized surface plasmon resonance sensing properties of photocatalytically prepared Au/TiO_2 films. *Mater. Lett.* **62**, 2714 (2008).
10. K.L. Kelly, E. Coronado, L.L. Zhao, and G.C. Schatz: The optical properties of metal nanoparticles: The influence of size, shape, and dielectric environment. *J. Phys. Chem. B* **107**, 668 (2003).

11. J.J. Mock, M. Barbic, D.R. Smith, D.A. Schultz, and S. Schultz: Shape effects in plasmon resonance of individual colloidal silver nanoparticles. *J. Chem. Phys.* **116**, 6755 (2002).
12. N. Félidj, J. Aubard, G. Lévi, J. Krenn, M. Salerno, G. Schider, B. Lamprecht, A. Leitner, and F. Aussenegg: Controlling the optical response of regular arrays of gold particles for surface-enhanced Raman scattering. *Phys. Rev. B* **65**, 075419 (2002).
13. R. Jin, Y.C. Cao, E. Hao, G.S. Me, G.C. Schatz, and C.A. Mirkin: Controlling anisotropic nanoparticles growth through plasmon excitation. *Science* **425**, 487 (2004).
14. K. Matsubara, K.L. Kelly, N. Sakai, and T. Tatsuma: Plasmon resonance-based photoelectrochemical tailoring of spectrum, morphology and orientation of Ag nanoparticles on TiO_2 single crystals. *J. Mater. Chem.* **19**, 5526 (2009).
15. I. Tanabe, K. Matsubara, S.D. Stridge, E. Kazuma, and K.L. Kelly: Photocatalytic growth and plasmon resonance-assisted photoelectrochemical toppling of upright Ag nanoplates on a nanoparticulate TiO_2 film. *Chem. Commun.* **24**, 3621 (2009).
16. E. Kazuma, K. Matsubara, K.L. Kelly, N. Sakai, and T. Tatsuma: Bi- and uniaxially oriented growth and plasmon resonance properties of anisotropic Ag nanoparticles on single crystalline TiO2 surfaces. *J. Phys. Chem. C* **113**, 4758 (2009).
17. D.W. Li, L.J. Pan, S. Li, K. Liu, S.F. Wu, and W. Peng: Controlled preparation of uniform TiO_2-catalyzed silver nanoparticle films for surface-enhanced Raman scattering. *J. Phys. Chem. C* **117**, 6861 (2013).
18. R. Viswanatha, P.K. Santra, C. Dasgupta, and D.D. Sarma: Growth mechanism of nanocrystals in solution: ZnO, a case study. *Phys. Rev. Lett.* **98**, 255501 (2007).
19. A. Mills, G. Hill, M. Stewart, D. Graham, W.E. Smith, S. Hodgen, P.J. Halfpenny, K. Faulds, and P. Robertson: Characterization of novel Ag on TiO_2 films for surface-enhanced Raman scattering. *Appl. Spectrosc.* **58**, 922 (2004).
20. I.M. Arabatzis, T. Stergiopoulos, M.C. Bernard, D. Labou, S.G. Neophytides, and P. Falaras: Silver-modified titanium dioxide thinfilms for efficient photodegradation of methyl orange. *Appl. Catal., B* **42**, 187 (2003).
21. M.H. Ahmed, T.E. Keyes, J.A. Byrne, C.W. Blackledge, and J.W. Hamilton: Adsorption and photocatalytic degradation of human serum albumin on TiO_2 and Ag–TiO_2 films. *J. Photochem. Photobiol., A* **222**, 123 (2011).
22. L. Yang, X. Jiang, W. Ruan, J. Yang, B. Zhao, W. Xu, and J.R. Lombardi: Charge transfer induced surface-enhanced Raman scattering on Ag TiO2 nanocomposites. *J. Phys. Chem. C* **113**, 16226 (2009).
23. L.M. Sudnik, K.L. Norrod, and K.L. Rowlen: SERS-active Ag films from photoreduction of Ag^+ on TiO_2. *Appl. Spectrosc.* **50**, 422 (1996).
24. Y. Sakai, I. Tanabe, and T. Tatsuma: Orientation-selective removal of upright Ag nanoplates from a TiO_2 film. *Nanoscale* **3**, 4101 (2011).
25. I. Tanabe, K. Matsubara, N. Sakai, and T. Tatsuma: Photoelectrochemical and optical behavior of single upright Ag nanoplates on a TiO_2 film. *J. Phys. Chem. C* **115**, 1695 (2011).
26. A. Moores and F. Goettmann: The plasmon band in noble metal nanoparticles: An introduction to theory and applications. *New J. Chem.* **30**, 1121 (2006).
27. T. Ung, L.M. Liz-Marza, and P. Mulvaney: Optical properties of thin films of Au@SiO2 particles. *J. Phys. Chem. B* **105**, 3441 (2001).
28. M. Ohring: *Materials Science of Thin Films: Deposition and Structure* (Academic Press, San Diego, USA, 2002).
29. M. Niederberger and H. Cölfen: Oriented attachment and mesocrystals: Non-classical crystallization mechanisms based on nanoparticle assembly. *Phys. Chem. Chem. Phys.* **8**, 3271 (2006).
30. J. Zhang, F. Huang, and Z. Lin: Progress of nanocrystalline growth kinetics based on oriented attachment. *Nanoscale* **2**, 18 (2010).
31. S. Yin, F. Huang, J. Zhang, J. Zheng, and Z. Lin: The effects of particle concentration and surface charge on the oriented attachment growth kinetics of CdTe nanocrystals in H_2O. *J. Phys. Chem. C* **115**, 10357 (2011).
32. D.S. Li, M.H. Nielsen, J.R.I. Lee, C. Frandsen, J.F. Banfield, and J.J. De Yoreo: Direction-specific interactions control crystal growth by oriented attachment. *Science* **36**, 1014 (2012).